

## Sum energy technique for anti-neutrino event reconstruction in ISMRAN

S. P. Behera<sup>1</sup>, D. Mulmule<sup>1,2,\*</sup>, D. K. Mishra<sup>1</sup>,  
P. K. Netrakanti<sup>1</sup>, V. Jha<sup>1</sup>, L. M. Pant<sup>1,2</sup>, and B. K. Nayak<sup>1,2</sup>

<sup>1</sup>Nuclear Physics Division, Bhabha Atomic Research Centre, Mumbai - 400085, INDIA and

<sup>2</sup>Homi Bhabha National Institute, Mumbai - 400094, INDIA

### Introduction

Reactor anti-neutrino experiments primarily rely on the inverse beta decay (IBD) reaction to detect anti-neutrinos ( $\bar{\nu}_e$ ). In this reaction, a  $\bar{\nu}_e$  with IBD threshold energy of 1.806 MeV interacts with a proton in the detector volume, usually a scintillator, producing a positron and a neutron :  $\bar{\nu}_e + p \rightarrow e^+ + n$ . The Indian Scintillator Matrix for Reactor Anti-Neutrino (ISMRAN) proposed at Dhruva reactor facility in BARC, is one such experiment comprising of  $10 \times 10$  matrix of  $100\text{cm} \times 10\text{cm} \times 10\text{cm}$  plastic Scintillator (PS) bars wrapped with Gd ( $\text{Gd}_2\text{O}_3$ ) foil. In case of an IBD event in ISMRAN, the deposited energy due to ionization loss and annihilation of positron forms the ‘prompt’ event while energy deposited by de-excitation  $\gamma$ -rays after neutron capture on Gd forms the ‘delayed’ event. In this work we present the simulations performed to obtain the sum energy and bar multiplicity distributions of these prompt and delayed events distributions for the 100 PS bar ISMRAN setup. Results from measurements, using this approach to select  $^{60}\text{Co}$  source events from background in prototype matrix - mini-ISMRAN, are also presented.

### Reconstructed sum energy and multiplicity from simulation

Monte-carlo simulations are carried out using GEANT4 [1] to understand the sum energy and bar multiplicity ( $N_{\text{bars}}$ ) characteristics of IBD event in ISMRAN. These parameters are crucial as the energy deposition in PS

is not isolated to a single bar due to Compton scattering. Both the full ISMRAN geometry of 100 PS bars and 16 bar mini-ISMRAN with shielding of 10 cm Pb and 10 cm BP have been used in simulation. The parametrization of  $\bar{\nu}_e$  spectrum and relevant cross-sections are obtained from [2] and the references therein. A threshold  $E_{\text{bar}}^{\text{th}} > 0.2$  MeV on deposited energy in each PS bar, similar to that in data, is used in simulation. The sum energy distribution in

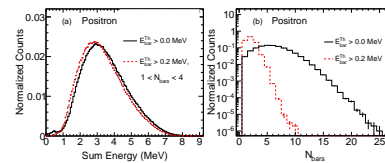


Fig 1: (a) The sum energy distribution in PS bars of the prompt positron events for  $E_{\text{bar}}^{\text{th}} > 0.0$  MeV and for  $E_{\text{bar}}^{\text{th}} > 0.2$  MeV with  $1 < N_{\text{bars}} < 4$  selection. (b) the corresponding  $N_{\text{bars}}$  distribution.

ISMRAN for each prompt positron event as shown in Fig 1(a) closely follows the  $\bar{\nu}_e$  spectrum above the 1.806 MeV threshold as most of the  $\bar{\nu}_e$  energy is carried by positron. The  $N_{\text{bars}}$  distribution for these events peaks at  $\sim 2$  and even extends to 10 bars in some of the events as seen in Fig 1(b). Most of the prompt events deposit energy within  $1 < N_{\text{bars}} < 4$ . The shift to lower energies due to  $E_{\text{bar}}^{\text{th}} > 0.2$  MeV and  $1 < N_{\text{bars}} < 4$  selection, on the prompt energy spectrum is also shown in Fig 1(a). This shift to lower values both in the reconstructed sum energy and  $N_{\text{bars}}$  is also observed for mini-ISMRAN geometry. It is observed in simulations that the delayed event i.e. neutron capture happens  $\sim 73\%$  of the time on Gd and  $\sim 25\%$  on H while remaining  $< 2\%$  on C and Pb. The sum energy distribution of delayed event, Fig 2(a), shows a distinct peak at

\*Electronic address: dhruvm@barc.gov.in

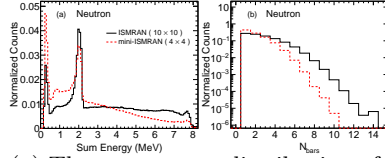


Fig 2: (a) The sum energy distribution of delayed neutron events with  $E_{\text{bar}}^{\text{th}} > 0.2$  MeV for ISMRAN and mini-ISMRAN setup with inside shielding (b) the corresponding  $N_{\text{bars}}$  hit distribution.

$\sim 2.0$  MeV of the H-capture  $\gamma$ -ray in both ISMRAN and mini-ISMRAN, indicating its almost complete containment. A low energy peak at  $\sim 0.3$  MeV is from the events where capture  $\gamma$ -rays escaping the sensitive volume, are scattered back from the shielding material. This feature is absent when the simulations are performed without any shielding material. Due to the  $E_{\text{bar}}^{\text{th}} > 0.2$  MeV as well as the limited geometrical acceptance of cascade  $\gamma$ -rays in ISMRAN the 8 MeV of sum energy is distributed over the entire energy range and reconstructed to even lower energies in mini-ISMRAN. The  $N_{\text{bars}}$  distribution, Figure 2(b), has maximum at 1 but also has significant events spanning multiple bars.

### Sum energy distributions for $^{60}\text{Co}$ source in mini-ISMRAN

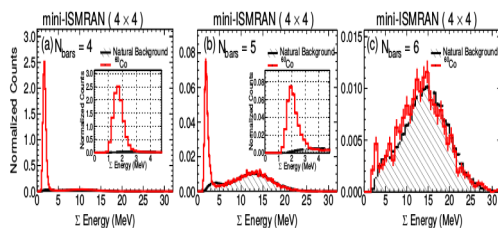


Fig 3: The sum energy distribution within 40 ns time window, (a)  $N_{\text{bars}}=4$ , (b)  $N_{\text{bars}}=5$  and (c)  $N_{\text{bars}}=6$ , for the  $^{60}\text{Co}$  and natural background events. The insets in panel (a) and (b) shows the peaks in  $^{60}\text{Co}$  sum energy zoomed-in.

Measurement with  $^{60}\text{Co}$  source placed inside mini-ISMRAN, in laboratory environment, is performed to study the feasibility of reconstructing coincident events. The source is placed at the center to maximize the containment of 1.17 MeV and 1.33 MeV coincident  $\gamma$ -rays of  $^{60}\text{Co}$ . Figure 3(a), (b) and (c) show the time normalized sum energy distribution from  $^{60}\text{Co}$  as well as natural

background data along with the condition of  $N_{\text{bars}}=4$ ,  $N_{\text{bars}}=5$  and  $N_{\text{bars}}=6$  hit, within a time window of 40 ns. Only those PS bars are selected for the sum energy where the individual energy deposit is below 7.5 MeV, to reduce the cosmic muon background. A peak at  $\sim 2$  MeV in Fig 3(a) and (b) corresponds to the coincident  $\gamma$ -ray events from  $^{60}\text{Co}$ . The reconstructed sum energy of the coincident event improves for  $N_{\text{bars}}=5$  case as compared to  $N_{\text{bars}}=4$ . The inefficiency in sum energy reconstruction is due to energy threshold  $E_{\text{bar}}^{\text{th}} > 0.2$  MeV on individual PS bars and the finite acceptance of mini-ISMRAN resulting in reconstruction of mean sum energies to values lower than 2.5 MeV. For  $N_{\text{bars}}=6$  condition, Figure 3(c), it can be seen the fraction of coincident events reconstructed from  $^{60}\text{Co}$  are reduced significantly as compared to the natural background events. Also it is observed that the ratio of signal from coincident events with  $^{60}\text{Co}$  to natural background events worsens with increase in  $N_{\text{bars}}$ . In all the three  $N_{\text{bars}}$  condition, the sum energy distribution above 5 MeV from both  $^{60}\text{Co}$  and natural background scales indicating the common source of background events.

### Conclusion and Outlook

The sum energy and multiplicity distributions obtained in simulations for both mini-ISMRAN and ISMRAN show that the  $N_{\text{bars}}$  selection of 2-3 bars for a prompt event and  $>3$  for delayed event will allow for prompt and delayed event separation and to filter out correlated  $\bar{\nu}_e$  signal from background. The measurement results from the sum energy study with  $^{60}\text{Co}$  source inside the mini-ISMRAN setup indicate that, by appropriately selecting  $N_{\text{bars}}$  and energy deposited in each PS bar the coincident events can be reconstructed in mini-ISMRAN.

### References

- [1] S. Agostinelli et al., GEANT4: A Simulation toolkit, Nucl. Instrum. Meth. A 506 (2003) 250.
- [2] Th. A. Mueller et al. Improved predictions of reactor antineutrino spectra. Phys. Rev. C, 83:054615, May 2011.